Composites Science and Technology

Shamsher Bahadur Singh
Madappa V. R. Sivasubramanian
Himanshu Chawla *Editors*

Emerging Trends of Advanced Composite Materials in Structural Applications

Springer

Composites Science and Technology

Series Editor

Mohammad Jawaid, Lab of Biocomposite Technology, Universiti Putra Malaysia, INTROP, Serdang, Malaysia

Composites Science and Technology (CST) book series publishes the latest developments in the field of composite science and technology. It aims to publish cutting edge research monographs (both edited and authored volumes) comprehensively covering topics shown below:

- Composites from agricultural biomass/natural fibres include conventional composites-Plywood/MDF/Fiberboard
- Fabrication of Composites/conventional composites from biomass and natural fibers
- Utilization of biomass in polymer composites
- Wood, and Wood based materials
- Chemistry and biology of Composites and Biocomposites
- Modelling of damage of Composites and Biocomposites
- Failure Analysis of Composites and Biocomposites
- Structural Health Monitoring of Composites and Biocomposites
- Durability of Composites and Biocomposites
- Biodegradability of Composites and Biocomposites
- Thermal properties of Composites and Biocomposites
- Flammability of Composites and Biocomposites
- Tribology of Composites and Biocomposites
- Bionanocomposites and Nanocomposites
- Applications of Composites, and Biocomposites

To submit a proposal for a research monograph or have further inquries, please contact springer editor, Ramesh Premnath (ramesh.premnath@springer.com).

More information about this series at http://www.springer.com/series/16333

Shamsher Bahadur Singh ·
Madappa V. R. Sivasubramanian ·
Himanshu Chawla
Editors

Emerging Trends of Advanced Composite Materials in Structural Applications

Springer

Editors
Shamsher Bahadur Singh
Department of Civil Engineering
Birla Institute of Technology and Science
Pilani, India

Himanshu Chawla
Department of Civil Engineering
Thapar Institute of Engineering
and Technology
Patiala, India

Madappa V. R. Sivasubramanian
Department of Civil Engineering
National Institute of Technology
Puducherry
Puducherry, India

ISSN 2662-1819 ISSN 2662-1827 (electronic)
Composites Science and Technology
ISBN 978-981-16-1687-7 ISBN 978-981-16-1688-4 (eBook)
https://doi.org/10.1007/978-981-16-1688-4

This Springer imprint is published by the registered company Springer Nature Singapore Pte Ltd.
The registered company address is: 152 Beach Road, #21-01/04 Gateway East, Singapore 189721, Singapore

Contents

Composite Behaviour of Thin Precast Concrete Sandwich Panels

Roger P. West and Oliver Kinnane

Abstract This chapter discusses the composite behaviour of thin wythe precast concrete sandwich panels comprising sustainable mixes, hybrid fibres and non-conductive shear connectors. Following a review of available high performance concretes, insulation and shear connector types, it focuses on the individual and collective load-deflection behaviour of insulation, single wythes, unconnected and connected wythes with short and long spans under flexural loading where both grid and pin fibre reinforced polymer shear connectors are used to assist in developing better composite action. It concludes that, depending on insulation thickness and stiffness and connector type, partial composite action can be achieved in enhancing the ultimate load capacity of precast concrete sandwich panels.

Keywords Facades · High performance concrete · Precast concrete · Sandwich panels

1 Introduction

In the context of the absolute imperative to reduce the carbon footprints associated with the construction and operation of buildings, which accounts for about 40% of carbon dioxide emissions worldwide (Directorate General for Energy 2017), the criticality of the manufacture, construction and structural and thermal performance of façades in use is acute. The significant majority of domestic and commercial buildings are energy inefficient in terms of heating or cooling demands in delivering occupant comfort and the use of conventional concrete in the building envelope

R. P. West (✉)
Department of Civil, Structural and Environmental Engineering, Trinity College, University of Dublin, Dublin 2, Ireland
e-mail: rwest@tcd.ie

O. Kinnane
Architecture, Planning and Environmental Policy, University College Dublin, Belfield, Dublin 2, Ireland
e-mail: oliver.kinnane@ucd.ie

S. B. Singh et al. (eds.), *Emerging Trends of Advanced Composite Materials in Structural Applications*, Composites Science and Technology,
https://doi.org/10.1007/978-981-16-1688-4_1

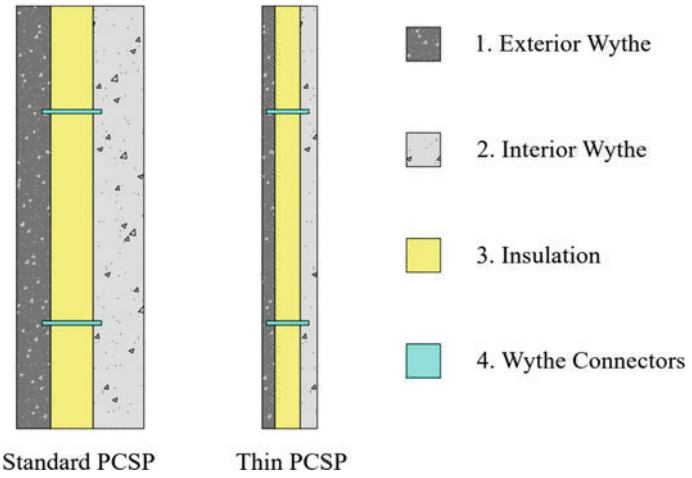

Fig. 1 Typical thick and thin PCSPs (O'Hegarty et al. 2019)

is not sustainable (Kinnane et al. 2014). However, as shall be discussed here, the evolution of more sustainable high performance thin lightweight precast concrete sandwich panels (PCSP) has the potential to have a significant impact on the cladding, re-cladding and over-cladding of new and existing building stock (FIB 2017).

Well-established thick heavy sandwich panels comprise an inner leaf, or wythe, and a thinner water-resistant outer rain screen wythe, infilled with insulation and connected by some form of shear connector, usually concrete webs or steel plates (Fig. 1). Panels are traditionally steel reinforced and structurally load-bearing, resisting wind, dead and live loads including self-weight, often with steel shear connectors (Kinnane et al. 2020). Typically 300–400 mm wide and weighing of the order of 500 kg/m^2, they impose considerable loads on lower floor columns and foundations.

However, in the provision of non-load bearing over-cladding or re-cladding facades, there has been considerable progress in reducing the inner and outer wythe thicknesses through the utilisation of high performance and more sustainable concrete, more efficient and/or greater thicknesses of insulation and non-conductive shear connectors to reduce the self-weight loads while aiming to provide the requisite structural strength and improved thermal performance (O'Hegarty and Kinnane 2019). Herein lies the main challenge—how to provide sufficient composite action between two thin high strength concrete wythes which accommodate larger insulation thicknesses using non-conductive connectors which transfer shear adequately between the wythes. In essence the aim is to maximise structural efficiency through composite action in conjunction with low thermal transmittance and minimal thermal bridging.

This is unobtainable without using innovative concrete composites containing alternative non-corrosive reinforcement, low thermal conductivity insulation and

effective mechanical connectors such that partial composite action is achieved. This chapter will discuss how this might be successfully accomplished.

2 PCSP Elements

2.1 Concrete Wythes

In thick PCSPs, made using normal strength concrete (with water to cement ratios (w/c) of the order of 0.4–0.6), durability issues and the need for cover to the reinforcing steel bars drive up the minimum wythe thickness. For thin wythes, where the strength must be much higher, alternative concrete types are needed and there are many choices, some of which, with their abbreviations, are listed in Table 1. For more sustainable mixes, supplementary cementitious materials (SCMs) either partially or fully replace the less sustainable normal Portland cement (NPC), particularly the pozzolans: fly ash (FA), ground granulated blast-furnace slag (GGBS) and silica fume (SF). The latter is particularly used for high performance or ultrahigh performance concrete (HPC or UHPC) as it is very fine, chemically reactive and helps fill the natural voids in the cement matrix.

To have a viable HPC or UHPC with the high flexural strength needed by PCSPs, the w/c ratio must be low (circa 0.25–0.3) which, with a high cement content, means that there will be a much lower quantity of capillary voids (those water or air filled voids formed by virtue of surplus water not needed to hydrate all of the cement present). The higher strength of the cement matrix also bonds more effectively with the shear connectors. Often small diameter coarse aggregates only are used, with a void filler to particle pack the mix, minimising the void content, reducing porosity and improving compressive and flexural strength and durability. To maintain workability, a superplasticiser is essential, with long mixing times. Assuming good mechanical compaction and curing, the high strength thus attained creates a more brittle concrete which is also vulnerable to shrinkage cracking, both of which can be overcome by adding fibres. The type, size and dosage of fibre depends on the required properties, but principally they are added to control cracking and add flexural toughness post-cracking, when the elastic limit of the concrete is exceeded. In sufficient dosage, the fibres bind the concrete together, distribute the cracks and prevent them from opening under increasing load and/or displacement in a standard prism flexural test and in the panels themselves.

A series of typical mixes are given in Table 2 for illustration. Mix A is a mix with limestone aggregate which could be used for a thick wythe, where, for example, an NPC (or European CEM I) mix with a w/c ratio of 0.53 delivers cube compressive and beam flexural strengths of 37 and 6.9 MPa, respectively at 28 days. By increasing the cement content from 400 to 610 kg/m^3, with SCMs of GGBS and SF and 400 kg/m^3 of a calcium carbonate filler, the w/c of 0.33 delivers 89 and 13.3 MPa compressive and flexural strengths, respectively. By adding a high dosage of hybrid fibres, these

Table 1 Some concrete types for thin wythe PCSPs

Abbrev.	Name	Description
OPC/NPC	Ordinary/normal Portland cement concrete	Concrete containing traditional Portland cement as binder
FC	Foamed concrete	Low strength with no stone and highly voided to improve thermal properties
SCC	Self-compacting concrete	Highly fluid but sufficiently viscous to avoid segregation and requires no compaction
FRC	Fibre reinforced concrete	Contains one or two types (hybrid) of fibres to enhance crack control and post-cracking toughness
GRC	Glass-fibre reinforced concrete	Glass fibres added to mix, short or long, for shrinkage cracking resistance
SFRC	Steel fibre reinforced concrete	Steel fibres of different shapes and aspects ratios added to mix for shrinkage, cracking control and toughness
RCA	Recycled concrete aggregate	A more sustainable mix where old concrete has been crushed to a given size
RPC	Reactive powder concrete	High quantity of very fine cement without stone
GC	Geopolymer concrete	NPC is replaced by supplementary cements, usually pozzolans, activated by chemicals
PCMC	Phase-change material concrete	Solid granules added to mix to enhance the thermal storage capacity, while reducing strength
TRC	Textile reinforced concrete	A fabric or textile of different composition added to act as reinforcing
HPC	High performance concrete	Any concrete with compressive cube strength above 80 MPa
UHPC	Ultra-high performance concrete	Any concrete with compressive cube strength above 125 MPa. May or may not include fibres
UHPFRC	Ultra-high performance fibre reinforced concrete	A combination of any UHPC with FRC

strengths rise to 97 and 15.5 MPa, respectively. To make the concrete more sustainable still, supposing a recycled concrete aggregate (RCA) replaces the virgin limestone aggregate in full. It would be expected that the strengths would drop because the surfaces of the RCA contain porous adhered cement paste which is normally weaker and more absorbent than the parent limestone aggregate and so it is the case that the strengths drop to, for example, 80 and 11.0 MPa, respectively. To overcome this, a lower w/c of 0.25 is used together with additional SF to pre-coat (and thus block) the voids on the RCA, whereupon the strengths rise to 90 MPa and 13.5 MPa,

Table 2 Typical wythe concrete mixes: A: control (limestone); B: HPC limestone; C: HPFRC limestone; D: HPFRC RCA; E: HPFRC RCA + SF (Lipszynska et al. 2020)

Mass in kg/m^3	A	B	C	D	E
CEM I cement	400	254	254	254	254
GGBS	0	254	254	254	254
SF	0	102	102	102	109
10 mm crushed limestone	1050	760	760	0	0
10 mm recycled concrete aggregate	0	0	0	760	760
Fine aggregate	700	715	715	715	715
Calcium carbonate filler	0	400	400	400	400
Water	210	200	200	200	154
Superplasticiser	0	18	18	18	18
Steel fibres (30 mm)	0	0	39	39	39
Polypropylene fibres (24 mm)	0	0	18	18	18
w/c ratio	0.53	0.33	0.33	0.33	0.25
Cube strength (MPa)	37	89	97	80	90
Flexural strength (MPa)	6.9	13.3	15.5	11.0	13.5

respectively, representing a viable and more sustainable fibre reinforced HPC in the manufacture of thin wythes for use in PCSPs.

To observe the effect of fibres in term of enhancing strength and post-cracking toughness, Fig. 2 demonstrates that a HPC without fibres has a brittle response with flexural (tensile) and compressive strengths of 9.4 and 99.6 MPa, respectively, while a mix with 2.9% of 24 mm alkali resistant glass fibres added has a flexural strength of 15.3 MPa, with a compressive strength of 96 MPa (with a modulus of elasticity of 49.6 GPa). The considerable toughness post cracking (at circa 9.2 MPa) and residual strength post peak are notable. These properties are essential for PCSPs when subject to extreme wind or impact loading.

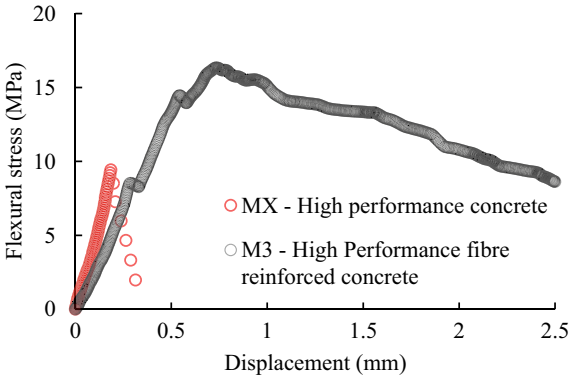

Fig. 2 Flexural test results on a 160 × 40 × 40 prism of HPC with and without 2.9% of 24 mm glass fibres (O'Hegarty et al. 2020)

2.2 Insulation

The primary purpose of insulation in a PCSP is to provide thermal resistance across the façade element. Usually building standards specify a maximum thermal transmittance or U-value, which is the inverse of the sum of the resistances of each of the components of the façade through the thickness. There is a trade-off between the coefficient of thermal conductivity, k, and the thickness of the insulation layer needed to meet the standard. Table 3 lists some of the more common insulation types, from the more conductive (concrete) to the least conductive (VIP), with typical k values. While the VIP insulation is highly thermally efficient, it is also prohibitively expensive. The mineral wool insulations are highly compressible and so are unsuitable for PCSPs.

Figure 3 shows the different panel thicknesses which arise when VIP (30 mm thick), PF (110 mm) and EPS (180 mm) are used to deliver a U-value of 0.18 W/m K with 80 mm inner and outer concrete wythes. However, in the context of optimising the composite structural action between two wythes, the further apart the wythes become, as necessitated by the insulation choice for a given thermal performance, the more work the shear connectors have to do, recognising also that the compressive and flexural resistance of the insulation can also contribute to the load resistance of a PCSP.

The insulation and shear connectors can both offer compression resistance under lateral wind loads to promote load share between the two wythes and the concrete-insulation bond in longitudinal shear under flexure can also assist in enhancing the load carrying capacity to some degree. Figure 4, for example, shows the efficacy of XPS and EPS insulation in resisting compressive loads in a displacement control axial compression test (Fig. 5). It may be observed that after the short linear elastic region, continued crushing resistance is offered by the insulations such that a residual load capacity exists even under large displacements. The plots tail upwards as the bottom and top platens of the test machine engage.

Table 3 Different insulation types with indicative thermal conductivity coefficients, k

Abbrev.	Name	Thermal conductivity, k (W/m K)
–	Concrete	1.800
FC	Foamed concrete	0.500
MW	Mineral wool	0.038
EPS	Expanded polystyrene	0.037
XPS	Extruded polystyrene	0.030
PUR	Polyurethane foam	0.028
PIR	Polyisocyanurate	0.023
PF	Phenolic foam	0.021
VIP	Vacuum insulation panel	0.007

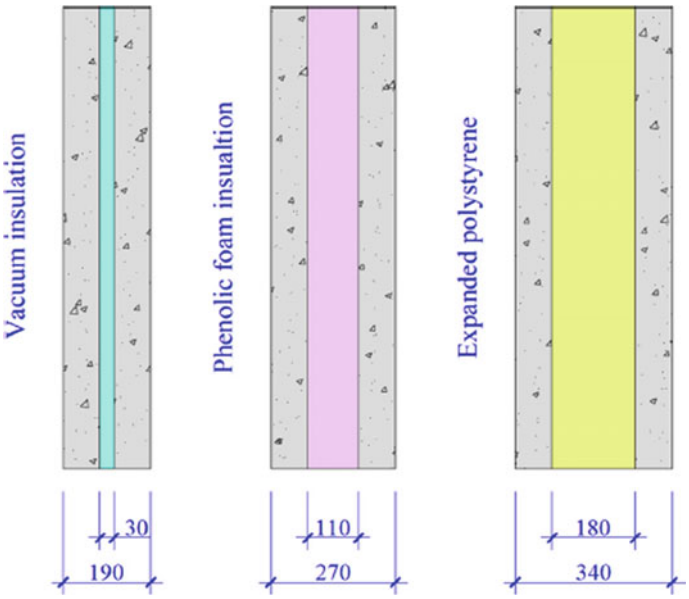

Fig. 3 Insulation thickness for a PCSP to satisfy a U-value of 0.18 W/m K using different insulating materials (O'Hegarty and Kinnane 2019)

Fig. 4 Compression test on EPS (left) and XPS (right) insulation sheets (Shukla 2019)

Similarly, Fig. 6 shows, from a flexural test on 5 sheets of plain XPS insulation siliconed together, that the insulation offers linearly increasing load capacity up to about 0.5 kN at about 30 mm displacement, indicating excellent flexibility in flexure.

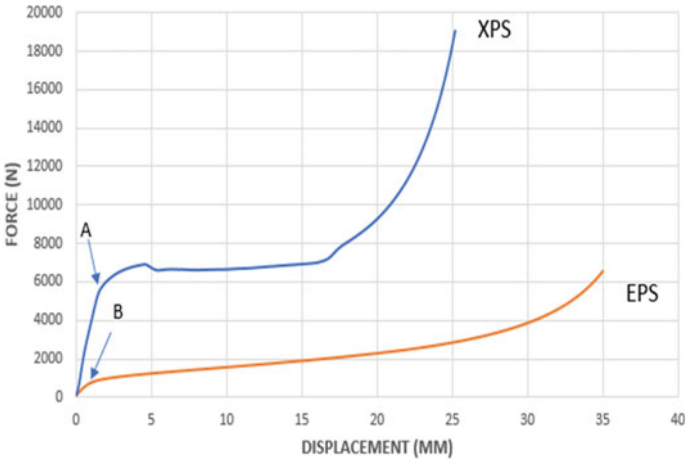

Fig. 5 Force-displacement plot for XPS and EPS insulation sheets (Shukla 2019)

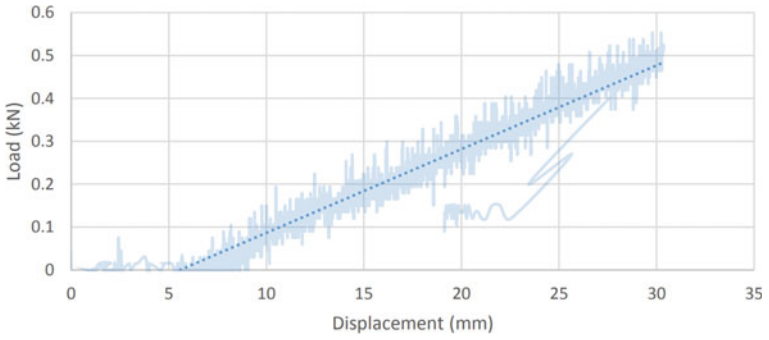

Fig. 6 Load–displacement plot for the flexural testing of 5 sheets of XPS insulation (180 mm thick) glued together using silicone (Lipszynska et al. 2020)

2.3 Connectors

The nature of the connection between the two wythes determines not only the structural but also the thermal performance of the PCSP. These connectors can be continuous, such as a vertical web of concrete or an FRP grid/truss, or can be discrete entities placed at the required centres in rows, such as steel plates or FRP pins (Fig. 7). The more conventional connectors, such as concrete or steel trussed bars or flat plates can be effective at developing good composite action, but have a significant drawback in their ability to create a thermal bridge between the outside and inside of a building due to their thickness (Fig. 7) and high thermal conductivity (see Table 4).

Furthermore, while most connectors have good to excellent tensile strength capacity (Table 4), their connector geometries also determine their susceptibility

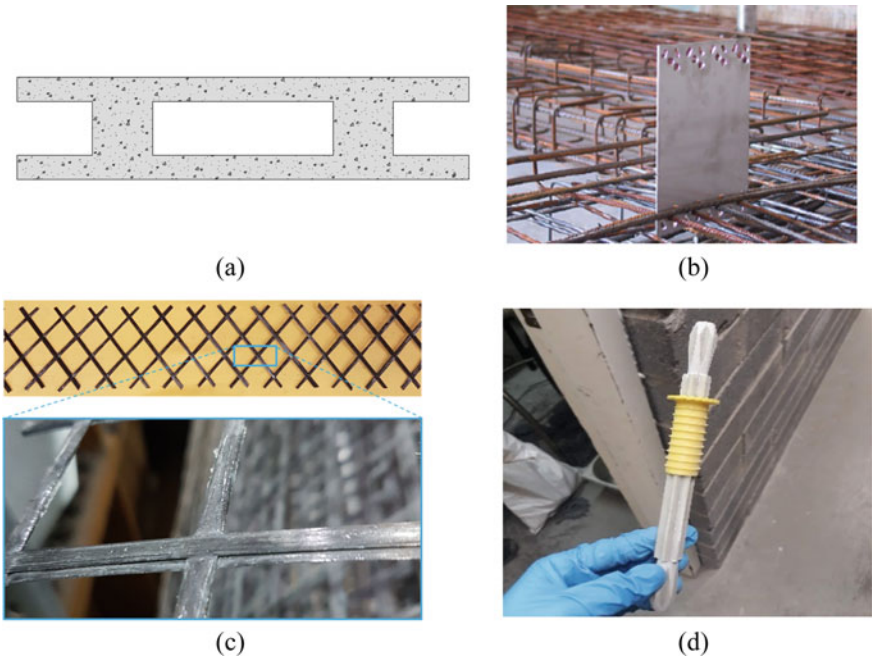

Fig. 7 Examples of **a** concrete web (O'Hegarty et al. 2020), **b** steel plate (Kinnane et al. 2020), **c** CFRP truss (O'Hegarty et al. 2020) and **d** FRP pin connectors (Lipszynska et al. 2020)

Table 4 Indicative properties of different connector types (O'Hegarty and Kinnane 2019)

Abbrev.	Name	Tensile strength (MPa)	Young's modulus (GPa)	Thermal conductivity, k (W/m K)
–	Ultra high strength concrete	12 MPa	40	2
–	Steel plates	450–700	200	50
CFRP	Carbon fibre reinforced polymer	600–3700	120–580	5–8
GFRP	Glass fibre reinforced polymer	480–1600	35–50	0.3–1
BFRP	Basalt fibre reinforced polymer	1100	70	1

to buckle under compression, such as in thin plates or CFRP grids or trusses in lateral shear. For example, the compressive and tensile responses of CFRP grids when embedded in a rigid foam is exemplified in Fig. 8 in which the spacing of the grid matrix affects tensile strength while the compressive strength is negligible, noting the change of axis scale in the compressive zone in the graph. What this

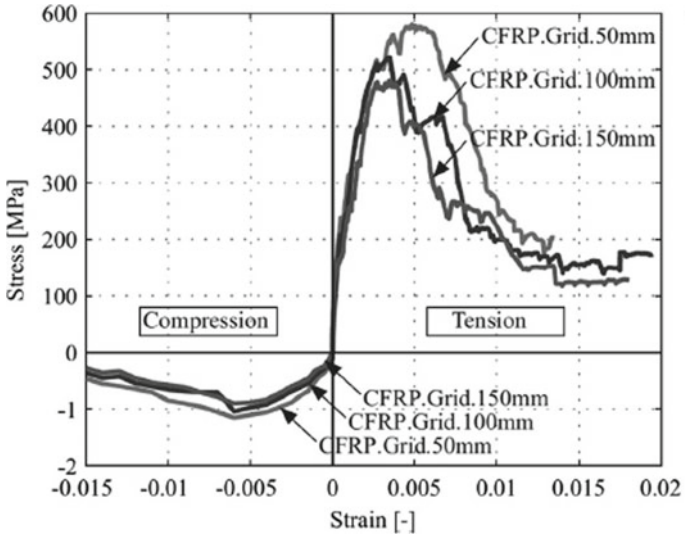

Fig. 8 Behaviour of CFRP grids within rigid foam subject to pure tension and compression (O'Hegarty and Kinnane 2019)

implies in practice is that the insulation becomes a key factor in determining the elastic composite behaviour of PCSPs made with such connectors—the lateral shear is resisted by a virtual truss in which alternate members of a CFRP truss act in tension while the insulation acts in compression due to the inability of the CFRP to resist compressive forces without buckling. Therefore, in addition to the spacing and orientation of the connectors, the insulation stiffness and width can also affect the composite behaviour of the PCSP.

On the other hand, the FRP pins (Fig. 7d), while much more effective at transferring compressive loads from an outer to an inner wythe in the transverse direction, are poor at resisting lateral shear forces parallel to the plane of the wythes. These matters will be explored further in due course using case studies.

3 Determining the Extent of Composite Action in PCSPs

Considering a single wythe of a PCSP, the thermal efficiency is determined by the thermal resistance (= 1/U value) which is proportional to the thickness, t, while the structural efficiency is determined by t^3 where t is the wythe thickness. If there are two wythes which are joined by connectors which are incapable of transferring lateral shear but can transfer applied load, such as through non-bonded insulation or isolated FRP pins, then the relative flexural stiffnesses of the wythes will determine the load share, as illustrated in Eqs. 1–3 in Table 5 and Fig. 9. This scenario represents

Table 5 Equations to calculate the second moment of area, I, of fully composite and non-composite PCSPs, with dimensions defined in Fig. 9 (O'Hegarty et al. 2019)

Non-composite panel		Fully composite panel	
$I_1 = \frac{b_1 t_1^3}{12}$	(1)	$A = b(t_1 + t_2)$	(4)
$I_1 = \frac{b_2 t_2^3}{12}$	(2)	$c_1 = \frac{[0.5bt_1^2 + bt_2(h - 0.5t_2)]}{A}$	(5)
$I_{nc} = I_1 + I_2$	(3)	$I_c = \frac{bt_1^3}{12} + bt_1 y_1^2 + \frac{bt_2^3}{12} + bt_2 y_2^2$	(6)

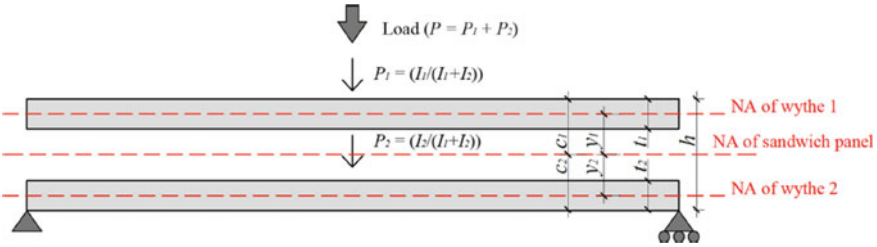

Fig. 9 Relevant dimensions and neutral axes for a PCSP for composite and non-composite cases, showing load share depending on the second moment of area of wythes if non-composite (O'Hegarty and Kinnane 2019)

non-composite action, as illustrated in Fig. 10b in which the individual wythes bend about their own neutral axes.

If, in contrast, in full composite action (Fig. 10a), there is complete transfer of shear between the two wythes, then the second moment of area, I_c, increases very substantially, as illustrated in Eqs. 4–6 in Table 5 and stresses and deflections are considerably smaller under identical loads. The additional terms involving the distance of the centroid of each wythe from the neutral axis (y_1 and y_2) contain a square term and so dwarf the t^3 term due to bending about the thin individual wythe's neutral axes. Therefore, the further apart the wythes are, the greater the structural efficiency if

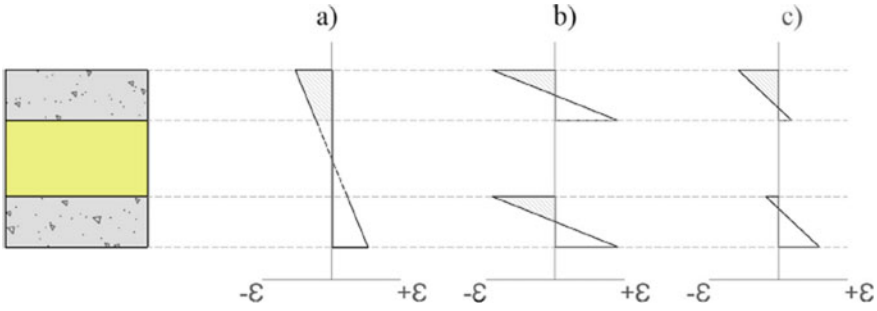

Fig. 10 Degree of composite action displaying approximate strain plots for **a** fully composite, **b** non-composite and **c** partially composite action (O'Hegarty and Kinnane 2019)

there is composite action. However, the further apart the wythes, the harder it will be for the shear connectors to develop full composite action and partial composite action (Fig. 10c) is more likely. For a given insulation/wythe/connector type, the wider the cavity the insulation fills, the better the thermal efficiency but only in proportion to the cavity width. So there is an incentive to increase the cavity width to improve the U value, but at a potential cost of structural efficiency and thus a balance must be found, especially if the connectors become less effective at transferring lateral shear.

The degree of partial composite action can be determined by assessing the elastic load-deflection response in a flexural test to establish the actual second moment of area being achieved in practice, comparing this to the full composite and non-composite theoretical values, as determined by Eq. (7) (O'Hegarty et al. 2020). The effective second moment of area is calculated from a three point flexural test value for deflection using Eq. (8) (O'Hegarty et al. 2020).

$$k(\%) = \frac{I_{exp} - I_{nc}}{I_c - I_{nc}} \tag{7}$$

$$EI_{exp} = \frac{PL^3}{48\delta} \tag{8}$$

In terms of testing a PCSP in flexure, although four point loading is often used, given there is a particular interest in lateral shear, the bending moment diagram for four point loading (Fig. 11) has two disadvantages: there is no shear in the central third of the beam and the moment in the central third is a constant, leading to more variable results due to the wider area over which flexural tensile cracking is likely to occur. Therefore, in the tests described here, they will all be conducted using three point loading, for which Eq. (8) applies. In practice, a uniformly distributed wind load is a common loading condition on a PCSP, so if, say, the wind pressure is 1.6 kPa, then on a span of 3.4 m, a PCSP has to resist a moment of 2.3 kN m to remain elastic. Therefore, the PCSP being tested must have a first cracking capacity of at least this magnitude.

Furthermore, it is normal when testing fibre reinforced concrete beams to use displacement control—that is, a displacement is imposed on the beam at a given

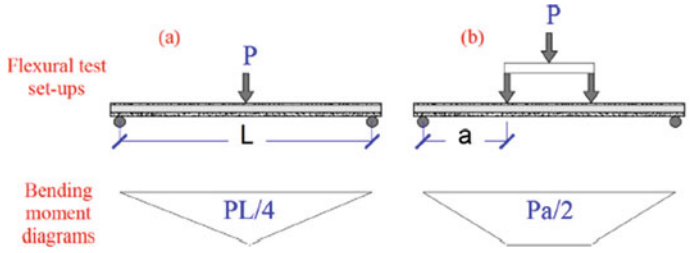

Fig. 11 Bending moment diagrams for **a** three and **b** four point flexural tests (O'Hegarty and Kinnane 2019)

rate (in mm per minute) so that the post-cracking toughness of the composite can be observed as the fibres pull-out of the cement matrix, such as observed in Fig. 2. The recorded load in such tests is the load resistance offered by the beam to that imposed displacement. If a load control test were to be used instead, then when the peak load is reached, the actuator would attempt to apply the next increment in load (at a given rate in kN/min), the beam would not have the capacity to resist such a load and failure would be sudden as the actuator head extension accelerates in an attempt to reach the next load increment. Therefore, there would be no post-cracking response in such cases. Hence, all the flexural results reported on here will be for displacement control tests.

Finally, there is a difference in the response of short or long span PCSPs because, under a given central point load, the transverse shear forces will not vary with span, whereas the bending moment and deflection will depend on the span (in proportion to L and L^3, respectively). Hence, in testing short span panels, the shear effects are exaggerated compared to the deflections and so present a sterner test of the shear force transfer capacity of the connectors.

4 Flexural Tests on Short Span PCSPs

4.1 Single Wythe Response

Using Mix C from Table 2 to create a single 900 × 600 × 20mm wythe in a simply supported flexural test with a central line load arrangement (Fig. 12), the load displacement graph in Fig. 13 demonstrates the initial linear response (to point A) followed by post-cracking ductility as the steel fibres gradually pull out (at B and C in particular), up to almost 40 mm central displacement, whereupon the slab rests on the lower platen causing an upward surge in the load. Strain gauge G2 (on the bottom of the wythe, see Figs. 12 and 14) also confirms the ability of the wythe to increase strain while sustaining load resistance capacity as the displacement is imposed incrementally. A further test was undertaken on a slab with two 35 × 35 mm ribs (used

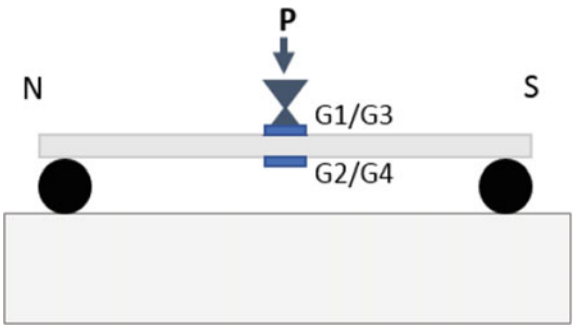

Fig. 12 Single wythe flexural test (Lipszynska et al. 2020)

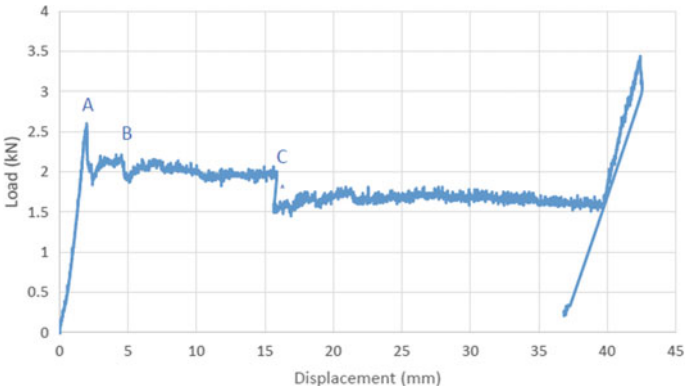

Fig. 13 Load versus mid-span displacement for single unribbed wythe in flexure (Lipszynska et al. 2020)

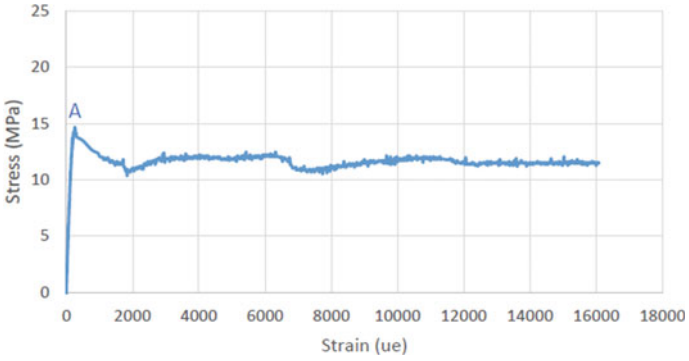

Fig. 14 Stress versus microstrain (G2) for single unribbed wythe in flexure (Lipszynska et al. 2020)

to embed connectors in the wythes more deeply) running longitudinally, which had a slightly higher capacity but very similar toughness response. Even with a fully developed crack, the wythe did not collapse due to the binding nature of the steel fibres (Fig. 15).

4.2 Unconnected Panel Short Span Response

By way of example, the flexural response of a 900 × 600 mm plan by 180 or 195 mm deep PCSP with two different insulation types will be discussed. As Fig. 16 shows, there is a lower thick wythe, of depth 120 mm, which is lightly reinforced with 4 no. 12 mm diameter high tensile steel bars. The upper thin UHPFRC wythe of 30 mm has a mix similar to Mix C in Table 2. The wythes are not connected by shear connectors.

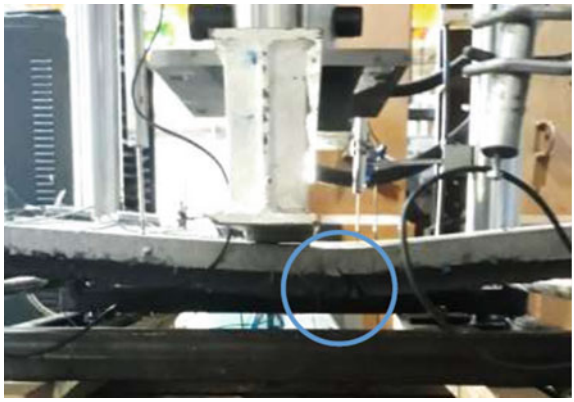

Fig. 15 Fully developed crack post-peak load for a ribbed single wythe (Lipszynska et al. 2020)

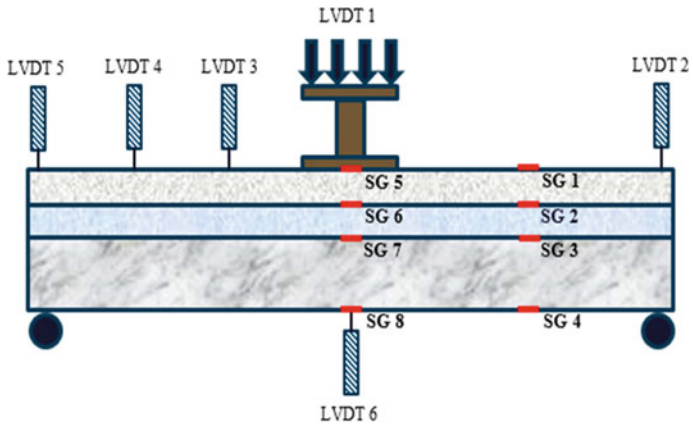

Fig. 16 Experimental set-up with strain gauges (SG) and displacement transducers (LVDT) locations (Shukla 2019)

The insulation is either 30 mm thick XPS or 45 mm of EPS, where the XPS initial stiffness is about 6 times that of the EPS (Fig. 5).

The influence of the insulation in the displacement response (over time, at a rate of 1 mm/min) of the unconnected PCSP may be observed from Fig. 17. Initially, the top wythe bends like a slab on an elastic foundation, where the lower wythe, which is much stiffer, provides relatively rigid support to the insulation, which helps to spread the load over the surface of the lower wythe. The upper wythe experiences its first crack at about point C in both XPS and EPS plots and, between points C and D, the ends of that wythe begin to lift, the crack widths under the load point increase, restrained by the fibres and a progressively smaller area of the outer edges of the insulation is engaged by the wythe as its edges lift progressively. From point D onwards, the insulation, under the V shaped rotated top wythe, is extensively compressed and the lower wythe now sustains almost all of the load in a simply supported slab

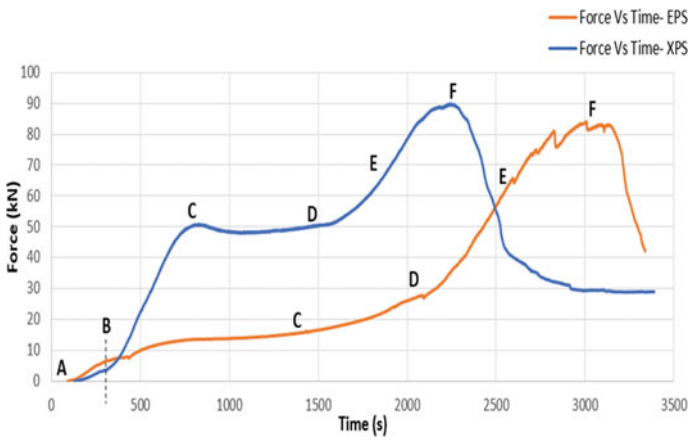

Fig. 17 Force versus time response in a flexural test on unconnected XPS and EPS insulated PCSPs (Shukla 2019)

arrangement. At point F, the reinforced lower wythe fails and the wythe's residual load capacity drops off substantially with continuing displacement. It may be observed that the insulation type plays a significant role in the responses, though peak load is determined by the bottom, stronger, wythe, at point F, as illustrated in Fig. 18. More importantly, from a serviceability viewpoint, there is a significant difference in the first crack load in the top wythe for the two insulation types due to the degree of flexure which arises in the top wythe, depending on the stiffness of the insulation.

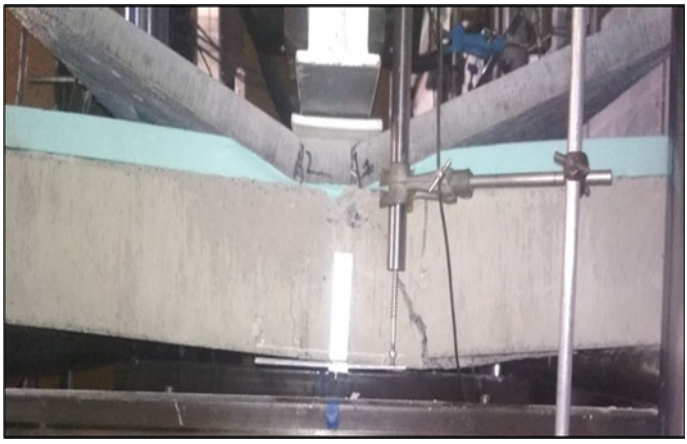

Fig. 18 Failure point of XPS insulated PCSP with top wythe disengaged (Shukla 2019)

4.3 Connected Short Span Thin Sandwich Panel Response

Consider a similar case but where a trussed CFRP grid (Fig. 7c) or discrete FRP pins (Fig. 7d) are used to connect the top and bottom wythes and with two sheets of siliconed XPS insulation.

As the load is applied, the early response for the trussed grid connector case is similar to the one above, where the grid provided very little compression resistance (Fig. 8) and a first crack appears on the bottom of the top wythe on either side of the load spreader (see Fig. 19a and the discontinuity in the curves in Fig. 20

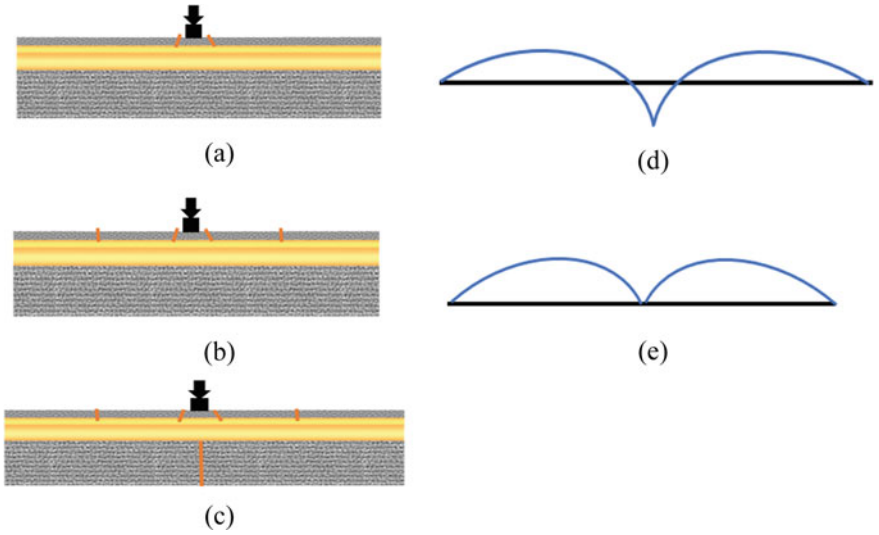

Fig. 19 Schematic of connected PCSP crack development (**a**–**c**) and the relevant bending moment diagrams for the top wythe (**d**, **e**) (Sexton et al. 2019)

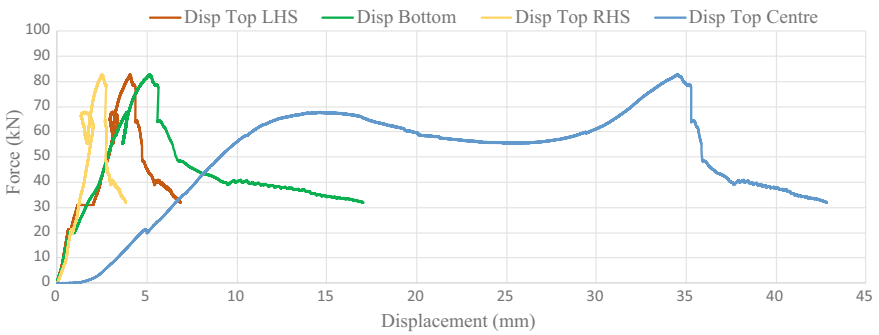

Fig. 20 Load displacement plot for the PCSP with XPS insulation and a trussed CFRP shear connector

at about 20 kN). This is because the bending moment diagram for a plate on an elastic foundation has peak sagging moment at the centre of the beam (Fig. 19d). The previous case showed that the edges now have a tendency to lift but the trussed connector resists this by developing a tensile force in response (see the top left hand (LH) and right hand (RH) curves in Fig. 20). At no point did the shear connector pull out of the 30 mm top wythe, suggesting that the bond with the UHPFRC was sufficient to embed the connector satisfactorily. An enhanced hogging bending moment ensues (Fig. 19e) which leads to tension on the top surface some distance from the load spreader, leading to a second pair of cracks propagating from the top surface of the top wythe (Fig. 19b) some distance either side of the load spreader. The top wythe continues to compress the insulation substantially as it moves downwards (see the top centre curve in Fig. 20). Ultimately, as further displacement is imposed in this displacement control test, the top wythe has little fibre pull-out resistance left and the lower wythe now takes all of the load until it too fails, at approximately 80 kN, by cracking in the centre of the bottom wythe (Fig. 19c). It should also be noted in Fig. 20 that the displacement at the centre of the bottom wythe (in green) is substantially less than the equivalent top wythe (in blue) under a given load because it is much stiffer as it is supported at its ends by a rigid vertical simply supported restraint, unlike the top wythe which is only supported by the highly compressible insulation. The resulting local crushing in the insulation in the vicinity of the load spreader at the point of failure of the bottom wythe may be observed in Fig. 21 in which the wythe ends may be observed as not having lifted due to the connector restraint.

In contrast, when a FRP pin shear connector is used, the pin can transfer the load more effectively to the bottom wythe as its axial stiffness is much higher than the insulation's. Therefore, as may be observed from Fig. 22, the top wythe displacements are considerably lower than the previous case and the local deformations near the spreader at the point of failure confirm this in Fig. 23. Figures 22 and 23 also confirm that the FRP pins are capable of resisting the uplift loads when the top wythe cracks (again at approximately 20 kN), with failure at approximately 80 kN as in the previous case.

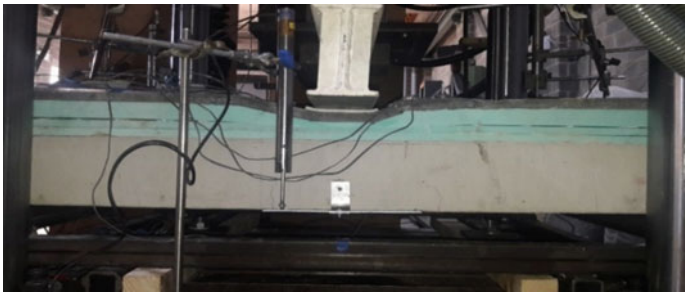

Fig. 21 The left and right wythe ends being restrained against uplift by the trussed CFRP connector in tension and insulation crushing under the load spreader due to local buckling of connector

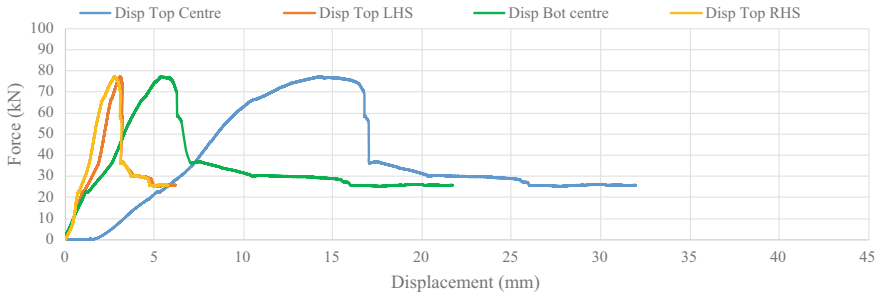

Fig. 22 Load displacement plot for the PCSP with XPS insulation and a pin FRP shear connector

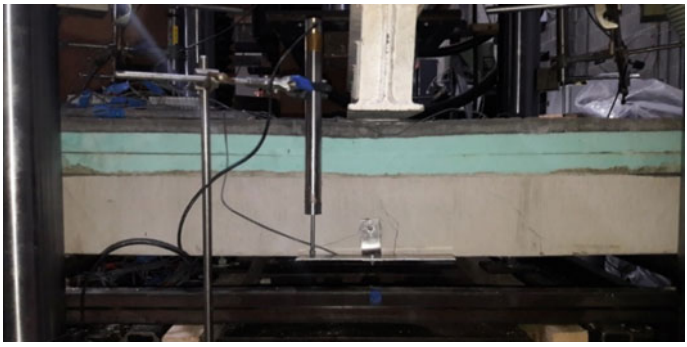

Fig. 23 The left and right wythe ends being restrained from lifting and insulation largely uncrushed under load spreader due to FRP pin connector

4.4 Connected Short Span Deep Sandwich Panel Response

With the desire for lighter, more thermally efficient PCSPs, the possibility of using a panel with two thin UHPFRC wythes and considerably greater insulation thicknesses pose additional challenges in developing composite action. Consider the case of a 900 × 600 mm panel with two 20 mm thick wythes with two 35 × 35 mm ribs along their length (Fig. 24) to accommodate the two rows of FRP pin shear connectors. The pins are 200 mm long so would only have 10 mm of embedment in each wythe were it not for the ribs. 180 mm of XPS insulation, in 5 siliconed sheets, was used, making a panel depth of 220 mm in total. The HPFRC concrete mix was highly sustainable with 50% GGBS, 100% recycled concrete as aggregate, coated with SF, and with hybrid fibres (mix E in Table 2). With a w/c of 0.25, the compressive and flexural strengths were 90 and 13.5 MPa, respectively (Table 2).

A finite element analysis of thick and thin bottom wythe panels under, say, a 50 kN point load with similar insulation thicknesses (Fig. 25) shows clearly that, in the linear elastic range, there is a significant difference in behaviour between the two cases. In case (a) the bottom wythe is so stiff that the top wythe flexes relatively

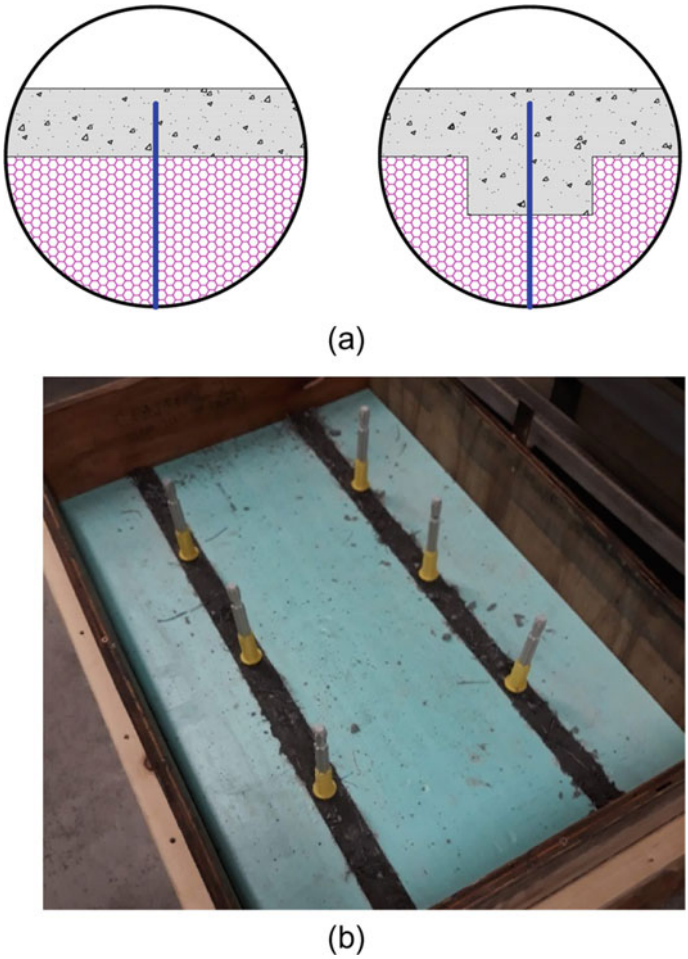

Fig. 24 **a** Graphic of 20 mm wythes with and without 35 mm ribs to enhance the anchorage of the shear connectors, used both top and bottom (O'Hegarty et al. 2020) and **b** the embedment of the FRP pin connectors at 200 mm centres between the two concrete panel pours in practice (Lipszynska et al. 2020)

so much more, giving rise to early cracking on the bottom face of that wythe, as observed previously (Fig. 19a). In case (b), with an equally thin bottom wythe, the stress on the bottom wythe can be greater (depending on the insulation and shear connector used) and so this lower wythe can crack first. One potential drawback of this is that if the panel is a vertical façade element, it is possible that the (unseen) inner wythe can crack without the outer wythe exhibiting any visible sign of distress, making the panel less safe under future loading. In practice, therefore, it is advisable to make the inner wythe slightly thicker than the outer one.

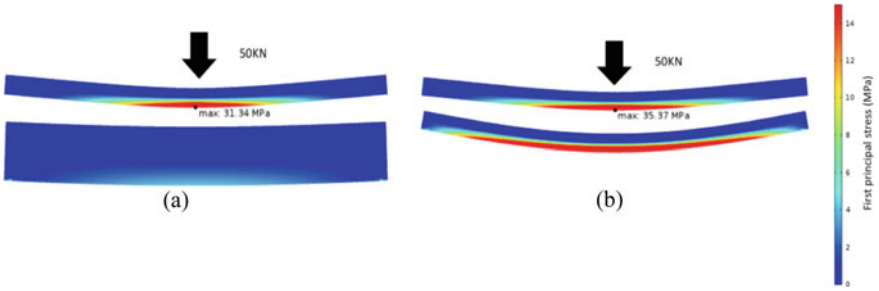

Fig. 25 Finite element elastic analysis leading to stress contours indicating a 50 kN load share for **a** thick and **b** thin bottom wythe PCSPs (O'Hegarty et al. 2018)

If two 220 mm thick ribbed panels are made up as described, one with and one without FRP pin connectors, with a simply supported test arrangement as before (Fig. 26), then the resulting load-deflection plots are as shown in Fig. 27a and b, respectively. In the unconnected case, as the panel is so deep, the top wythe and insulation leaves act as load spreaders and the bottom wythe cracks first at approximately the same load (2.5 kN) as a single wythe (Figs. 13 and 27a). Thereafter, with load resistance from the uncracked top wythe and the pull-out resistance of the bottom wythe, with a minor contribution from the insulation, the load resistance capacity increases to a second peak when fibre pull-out occurs in the lower wythe as the lower wythe cracks open up. The peak load (at D), when the top wythe develops a crack at about 3.5 kN, is somewhat less than the sum of the capacity of the two wythes (if they were load sharing equally). Thereafter, to point E, both fibre pull-out and shear slippage of the insulation leaves occur, with as much as 2 kN residual load capacity at failure. The physical state of the panel at this point may be observed in

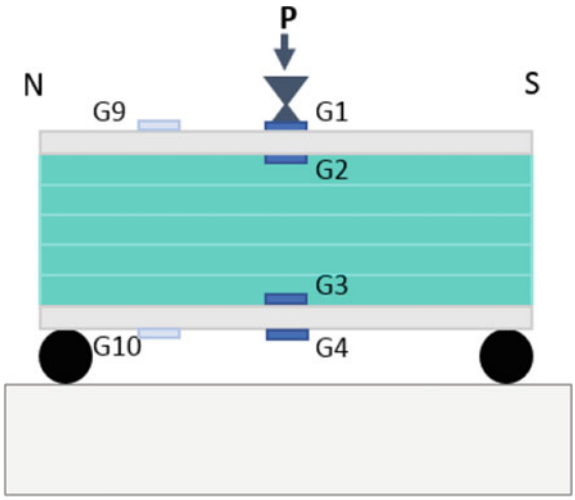

Fig. 26 Test set-up for unconnected and connected thin wythe deep PCSPs (Lipszynska et al. 2020)

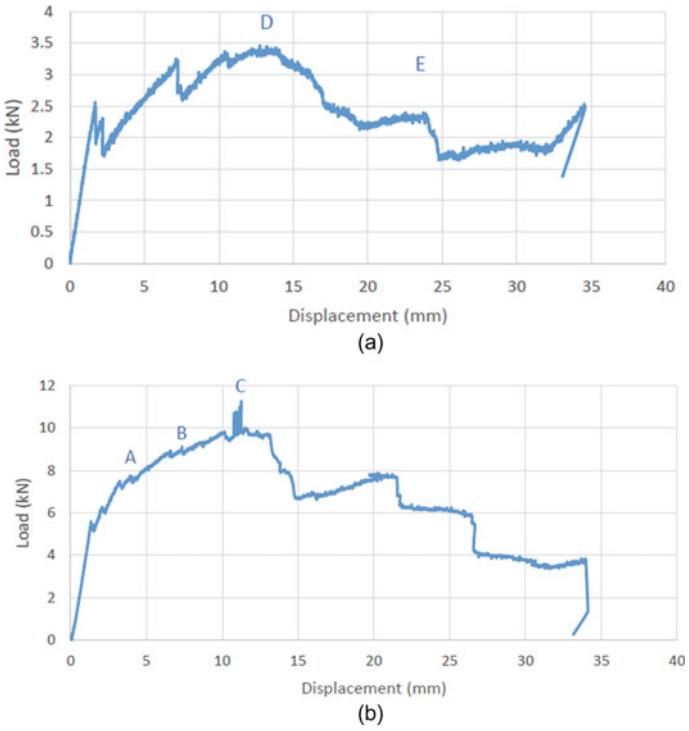

Fig. 27 Load mid-span displacement plots for **a** unconnected and **b** FRP pin shear connected PCSP made with sustainable UHPFRC panels (Lipszynska et al. 2020)

Fig. 28 in which the lower wythe is seen to be disengaged, the insulation sheets have slid horizontally (as may be observed from the staggered black vertical line on the insulation near the centre of the panel in the figure) and the top wythe has cracked but is holding the panel in place through the pull-out capacity of the fibres and the residual strength of the insulation (see also Fig. 6) which has not failed in tension despite the extent of sliding horizontally due to shear.

The connected panel has evidence of almost equal load share between panels at the point of the first crack at 5.5 kN (Fig. 27b) slightly more than twice the uncracked capacity of a single wythe.

The theoretical second moment of area of unconnected and fully composite arrangements are found to be 8×10^5 and 240×10^6 mm^4, respectively using Eqs. (1)–(6) from Table 5, the fully composite value being some 300 times the unconnected case. Using the single wythe test results (Fig. 13 and Eq. (8)) to estimate the modulus value, E, of the HPFRC as 35 GPa, the experimental composite value, I_e (Fig. 27b) can be estimated as 8.4×10^5 mm^4 from Eq. (8). Therefore the degree of partial composite action in the linear elastic range is calculated to be negligible (less than 0.1%), using Eq. (7), within experimental error.

Fig. 28 Unconnected thin UHPFRC wythe PCSP close to failure (Lipszynska et al. 2020)

Thus, there is no strong evidence here of composite action up to the elastic limit but, significantly, without evidence of a drop off in load due to wythe cracking, there is progression of load resistance from A to B until a peak at C of about 11.3 kN. It is reassuring that the post-cracking toughness during this displacement control test is such that the displacement at ultimate load is approximately 6 times that at the serviceability (first crack) limit.

The maximum load capacities of the insulation, single wythes with and without ribs, and the unconnected and connected panels are given in Table 6. It may be noted that the 11.3 kN capacity of the connected panel is approximately 50% higher than the sum of the individual peak capacities of the two wythes and insulation acting independently, indicating good composite action. The only difference between the two cases is the presence of the FRP shear pins which provides for this enhanced strength and the subsequent post-cracking toughness, with evidence of crack development and fibre pull-out in Fig. 27b. However, as the illustration of the final physical state of the panel shows in Fig. 29, the bottom wythe is again disengaged, the top has residual strength with restraint from the pull-out resistance of the steel fibres while the insulation shows much lower signs of slippage and subsequent tensile tearing

Table 6 Maximum load capacity of individual elements in thin UHPFRC wythes PCSPs (Lipszynska et al. 2020)

Element	Maximum load (kN)
Insulation	0.50
Wythe without ribs	3.44
Whythe with ribs	3.68
Unconnected thin wythe PCSP	3.46
Connected thin wythe PCSP	11.22